Punjab University Journal of Mathematics (2025), 57(12), 1324-1340
https:://doi.org/10.52280/pujm.2025.57(12)03

RBF-FD Method for Solving Generalized Burgers-Fisher Equation

Received
21 September, 2025

Revised
20 April, 2026
07 May, 2026

Accepted
14 May, 2026

Published Online
11 June, 2026

*Hameed Ullah Jan
Department of Mathematical and Statistical Sciences,
University of Science and Technology Bannu, Pakistan

Hafeez Ullah
Department of Mathematical and Statistical Sciences,
University of Science and Technology Bannu, Pakistan

Muhammad Rafiq
Department of Mathematical and Statistical Sciences,
University of Science and Technology Bannu, Pakistan

Zakia Qureshi
Department of Mathematical and Statistical Sciences,
University of Science and Technology Bannu, Pakistan,

Abstract.: Partial differential equations play a fundamental role in modeling nonlinear dynamical phenomena and are widely applied in fields such as fluid dynamics, solid-state physics, mathematical biology, and plasma physics. The generalized Burgers-Fisher equation is an important model that describes the interaction of diffusion, convection, and nonlinear reaction mechanisms in various physical systems, including traffic flow, heat conduction, and turbulence. In this paper, a local radial basis function-generated finite difference method is proposed for the numerical solution of the generalized Burgers-Fisher equation. The proposed method achieves high accuracy while requiring only a small number of nodes within a local stencil. Several numerical experiments are performed to validate the efficiency and accuracy of the method. The obtained results show excellent agreement with available analytical solutions and demonstrate the robustness of the proposed approach.

**Corresponding Author :* hameed_marwat@ustb.edu.pk

AMS (MOS) Subject Classification Codes: 35Q35, 65M70, 65M06, 65D15, 65M12.
Key Words: Generalized Burgers-Fisher (gBF) equation, Finite Difference (FD) method, Meshfree approach, Radial Basis Functions (RBF), RBF-FD method.

1. INTRODUCTION

Partial differential equations (PDEs) are widely used to describe a variety of natural phenomena, such as fluid motion, sound propagation, heat transfer, and wave propagation. Many important models in physics, fluid dynamics, electromagnetism, plasma physics, quantum mechanics, shallow water wave propagation, biology, and the social sciences can be described by PDEs, as shown in [20, 40]. Due to their broad applicability in physics, engineering, and other sciences, significant effort has been devoted to the numerical solution of PDEs alongside analytical studies. However, the development of highly accurate numerical methods and the validation of numerical results with experimental data remain active areas of research (see, for example, [23, 19]). Among nonlinear PDEs, the generalized BurgersFisher (gBF) equation is an important model that describes the combined effects of diffusion, convection, and nonlinear reaction mechanisms. This equation has significant physical relevance in modeling complex processes such as shock wave propagation, turbulence, heat conduction, and traffic flow. It is also used to study nonlinear wave phenomena and transport processes in viscous media. Recent studies further emphasize its importance in describing complex dynamical systems and nonlinear physical behavior [39, 43, 27]. The literature provides a variety of numerical techniques for approximating PDE solutions. Traditional methods include finite difference (FD), finite element (FE), and finite volume (FV) approaches, which rely on polynomial interpolation and typically achieve algebraic convergence rates. In contrast, global polynomial techniques, such as pseudo-spectral (PS) methods, can achieve exponential convergence but are limited by structured grids. Compared to spline-based methods such as B-splines, these traditional approaches also face limitations in handling irregular geometries and scattered data, since they generally depend on structured meshes and tensor-product constructions [22]. Moreover, these methods are not well suited for problems involving large deformations or irregular domains, where mesh generation becomes restrictive. In recent years, meshless methods have gained considerable attention, as they eliminate the need for mesh generation by employing scattered nodes over the problem domain. Notable examples include the local point interpolation method, reproducing kernel particle method, and the element-free Galerkin method [8, 31, 46].

Radial Basis Functions (RBFs) techniques have recently attracted considerable interest from the scientific community due to their truly mesh-free nature and their ability to provide spectral accuracy for PDE solutions on irregular domains [5, 10]. Hence, in situations where standard approaches are either difficult to apply or fail to achieve the desired exponential accuracy in multidimensional domains, global non-polynomial RBF methods can be effectively employed to obtain higher spectral accuracy. In addition to their superior accuracy and convergence rates compared to other advanced techniques, they also exhibit strong time-step stability, see for example [34, 31, 8]. The conventional RBF approach produces a full coefficient matrix due to globally defined basis functions. This limits its application to

large-scale problems, as the resulting matrix is often ill-conditioned. To address these limitations, Wendland et al. [45, 44] developed compactly supported RBFs. In addition, several authors have proposed local versions of RBF methods, which remain an effective alternative. The local approach aims to preserve the spectral accuracy of global techniques while generating a sparse and well-conditioned linear system suitable for large-scale problems. Another advantage of local techniques is their suitability for problems with discontinuous boundary conditions. The local radial basis function collocation method (LRBFCM) is one such local variant, as outlined by Chen in [7]. Instead of using all nodes in the computational domain for collocation, this method employs only local approximations [28, 30]. Among these approaches, the RBF-FD method is a particularly promising local strategy. It combines the advantages of RBFs with classical finite difference (FD) schemes to achieve high accuracy on scattered nodes without requiring a computational mesh. Wright and Tolstykh first introduced the RBF-FD method in 2000 [41, 47]. Furthermore, Bayona and Moscoso et al. [1] analytically established its convergence properties. In recent years, this approach has been successfully applied to a wide range of problems [28, 35, 13, 14, 15]. Although exact solutions are available for certain benchmark problems and are useful for validating numerical schemes, most real-world nonlinear partial differential equations do not admit closed-form solutions. Hence, numerical methods play a crucial role in obtaining accurate approximate solutions. In this context, the proposed RBF-FD method provides an effective framework for accurately approximating solutions where analytical solutions are unavailable, while maintaining high accuracy and computational efficiency. Moreover, the effectiveness of the proposed method is not solely based on numerical comparisons, but also on its meshless nature, reduced computational cost, and the use of local stencils, which produce sparse and well-conditioned systems.

The remainder of the paper is organized as follows. The details of the considered equations are given in Section 2, while the suggested schemes are described in Sections 3 and 4. The proposed systems stability evaluation is discussed in Section 5. Some numerical examples and results are presented in Section 6. Finally, comments and concluding remarks are given in Section 7.

2. GOVERNING EQUATIONS

The generalized Burgers-Fisher (gBF) equation is an important nonlinear partial differential equation that combines the physical properties of the Burgers equation and the Fisher reaction-diffusion equation to describe nonlinear phenomena involving simultaneous convection, diffusion, and reaction effects. The equation is commonly written as

$$\begin{cases} u_t + \alpha u^\delta u_x - \nu u_{xx} = \beta u(1-u^\delta), \text{ for } x \in [a,b] \text{ and } t \in (0,T], \\ u(x,0) = f(x), \text{ for } x \in [a,b], \\ u(a,t) = g_1(t) \text{ and } u(b,t) = g_2(t), \text{ for } t \in (0,T]. \end{cases} \tag{2. 1}$$

where the diffusion term νu_{xx} represents dissipative or spreading effects, the nonlinear convection term $\alpha u^\delta u_x$ models wave propagation and transport mechanisms, and the reaction term $\beta u(1-u^\delta)$ describes nonlinear growth-decay behavior. Physically, the gBF equation arises in several applications such as viscous fluid flow, gas dynamics, plasma physics, heat transfer, chemical kinetics, traffic flow, nonlinear acoustics, and biological population dynamics. The Burgers component models nonlinear transport and viscous

effects, while the Fisher component represents reaction-diffusion processes occurring in ecology, combustion theory, and biological systems. Due to its strong nonlinear characteristics and wide range of physical applications, the generalized Burgers-Fisher equation has become an important benchmark model for testing analytical and numerical methods in applied mathematics and engineering sciences [17, 2, 29, 36]. Furthermore, in equation (2. 1) $f(x)$ denotes the initial condition, while $g_1(t)$ and $g_2(t)$ represent the boundary conditions at the left and right boundaries, respectively. The parameters α, ν, δ, and β satisfy $\delta > 0$ and $\beta \geq 0$. The generalized Burgers-Fisher (gBF) model (2. 1) is investigated in the subsequent sections for different values of the parameters α, ν, δ, and β.

3. Description of the RBF-FD Method

3.1. **Classical Finite Difference Method.** To approximate the derivative of the function $u(x, y)$ with respect to x, we first consider a classical finite difference method. Assume that the derivative at each rectangular grid point (i, j) is approximated by

$$\frac{\partial u}{\partial x} \mid_{(i,j)} \approx \sum_{k \in \{i-1, i, i+1\}} w_{(k,j)} u_{(k,j)}. \tag{3. 2}$$

A stencil is defined in the finite difference literature as a set of nodes $\{(i-1, j), (i, j), (i+1, j)\}$, where $u_{(k,j)}$ denotes the function value at the grid point (k, j) and $w_{(k,j)}$ represents the unknown coefficients computed using Taylor series expansion or polynomial interpolation. The finite difference approximation of spatial derivatives relies on structured grids, which restricts its applicability in higher dimensions and reduces geometric flexibility [6]. Furthermore, in polynomial interpolation-based discretizations [48], the computation of finite difference coefficients for scattered nodes in multidimensional domains leads to a well-posedness issue, limiting the robustness of the method for irregular geometries.

3.2. **Radial Basis Function-Finite Difference Method.** To overcome the limitations of classical finite difference schemes, the radial basis function-finite difference (RBF-FD) method is employed as a mesh-free discretization approach [41, 47]. In this framework, the derivative of the function $u(x)$ at point x_i is approximated using a stencil, which is a local collection of nodes surrounding x_i. For each node, a stencil of neighboring points is selected, and differentiation weights are constructed by enforcing exactness over radial basis function interpolants. This leads to sparse differentiation matrices, improving computational efficiency while maintaining high accuracy. The method avoids the need for structured grids and provides flexibility for irregular geometries and scattered node distributions, making it suitable for high-dimensional problems [1].

4. Time-Dependent PDEs via the RBF-FD Method

To solve time-dependent PDEs, we provide a brief overview of RBFs and RBF-FD formulation. Consider the following time-dependent PDE:

$$u_t(x, t) = \mathcal{L}u(x, t), \text{ for } x \in \Omega \subseteq \mathbb{R}^d, \ d \geq 1, \text{ and } t \geq 0, \tag{4. 3}$$

subject to the following initial and boundary conditions

$$u(x, 0) = u_0(x), \text{ for } x \in \Omega, \ t = 0 \text{ and } \mathcal{B}u(x, t) = h(x, t), \text{ for } x \in \partial\Omega, \ t > 0, \tag{4. 4}$$

where u_0 and h are given functions, while $\mathcal{L}$ and $\mathcal{B}$ denote spatial differential operators. Consider $\Omega = \{x_1, \ldots, x_N\}$ as a discretized domain and $S^I = \{x_1^{(i)}, ..., x_{N_I}^{(i)}\} \subseteq \Omega$ be a stencil, consisting of N_I nodes associated with the point x_i, where $x_i \in S^I$ and $N_I \leq N$. Therefore, the linear differential operator $\mathcal{L}$ can be locally approximated as follows:

$$\mathcal{L}u(x_i) \simeq \sum_{j=1}^{N_I} w_j^{(i)} u(x_j^{(i)}). \tag{4. 5}$$

The problem of computing the unknown weights $\{w_j^{(i)}\}_{j=1}^{N_I}$ is solved by the RBF-FD approach, which requires that the linear combination (4. 5) for RBFs, $\{\phi_j(x,c)\}_{j=1}^{N_I}$, hold exactly true [48], centered at each stencil node S^I, so that

$$\mathcal{L}\phi_k(x_i,c) = \sum_{j=1}^{N_I} w_j^{(i)} \phi_j(x_k,c), \text{ for } k = 1, ..., N_I. \tag{4. 6}$$

The resulting algebraic linear system can be written as

$$\Phi \mathbf{w^I} = [\mathcal{L}\Phi]^I. \tag{4. 7}$$

The interpolation matrix $\mathbf{\Phi} \in \mathbb{R}^{N_I \times N_I}$ is defined as:

$$\phi_{kj} = \phi_j(x_k,c), \text{ for } k,j = 1, ..., N_I. \tag{4. 8}$$

The weight coefficients, also known as the RBF-FD coefficients, are $\{w_j^{(i)}\}_{j=1}^{N_I}$, which are contained in the $N_I \times 1$ coefficient vector $\mathbf{w^I}$, where the right-hand side vector $[\mathcal{L}\mathbf{\Phi}]^I \in \mathbb{R}^{N_I}$ contains entries $\mathcal{L}\phi_k(x_i,c)$ for $k = 1, \ldots, N_I$. Since the interpolant matrix $\mathbf{\Phi}$ is non-singular (see [33]), the weight vector $\mathbf{w}^I$ can be obtained. The discretization for problems (4. 3)-(4. 4) can be expressed as follows:

$$\mathbf{w}^I = \Phi^{-1}[\mathcal{L}\Phi]^I. \tag{4. 9}$$

The RBF-FD strategy is essentially an extension of the FD approach, with the exception of how the weights $\{w_j^{(i)}\}_{j=1}^{N_I}$ are established. It can therefore be considered an improved version of the FD approach. An analogous process can be applied to the boundary operator $\mathcal{B}$. Hence, after discretization, we obtain the following ODE:

$$\acute{u} = \mathbf{M}(u). \tag{4. 10}$$

The sparse differentiation matrix $\mathbf{M}$ of size $N \times N$ represents the discretized operator, indicating that each row contains n non-zero entries and $N - n$ zeros entries where n denotes the number of non-zero stencil points per row.

5. Stability of the proposed RBF-FD Numerical Scheme

In our proposed numerical scheme which is based on RBF-FD method we have transformed the time dependent partial differential equation into an ODEs system in time see equation (4. 10). This type of technique is called the method of lines by which we can solve this system of coupled ODEs using the finite difference method in time for example RK methods, etc. The method of lines stability may be estimated by the well known rule of thumb. It is shown in the work of [42], that the method of lines will be stable, when the eigenvalues of spatial discretization operator, linearized and scaled by step size δt, lie in

region of stability of the corresponding time-discretization operator. The stability region is a part of a multifaceted plane (complex plane) entailing of those eigenvalues for which the schemes construct a bounded solution. The stability of equation (4. 10) depends on the eigenvalues of the coefficient matrix. Hence, to show the stability of the numerical solution of equations (4. 3)-(4. 4), it is satisfactory to display that the real term of every eigenvalue $Re(\lambda_i)$of the matrix M is non-positive, i.e., $Re(\lambda_i) \leq 0$ for all $i = 1, 2, \cdots n$, for more details, see [38]. Notice that the traditional RK method of order four stability criteria is $(-2.78 < \lambda\delta t < 0 \forall \lambda)$. For more details on stability of RBF method for time dependent PDEs readers are refer to see for example [9, 25, 32]. Here in this study, it is shown that the current RBF-FD (localized) numerical scheme is unconditionally stable for all values of RBFs shape parameter and small step size δt, when solving the generalized Burgers-Fisher (gBF) equation.

5.1. **Time discretization using Runge-Kutta (RK-4) scheme.** The following system of ODEs is obtained using the spatial local RBF-FD approximation; that is, the PDE is converted into a system of ODEs:

$$D_t u = F(u). \tag{5. 11}$$

Any ODE solver, such as ode23, ode113, or ode45, can be applied to solve this system in time. The initial condition is given by u_0. To handle the stiffness of the ODE system, a suitable ODE solver automatically selects an appropriate time step δt. Alternatively, the fourth-order Runge-Kutta (RK-4) method can be used to solve the resulting ODE system. In this case, the time step δt is chosen manually.

RK-4 Scheme:

$$\mathbf{J_1} = \mathbf{F}(\mathbf{u^n}), \quad \mathbf{J_2} = \mathbf{F}(\mathbf{u^n} + \frac{\delta t}{2}\mathbf{J_1}), \quad \mathbf{J_3} = \mathbf{F}(\mathbf{u^n} + \frac{\delta t}{2}\mathbf{J_2}),$$

$$\mathbf{J_4} = \mathbf{F}(\mathbf{u^n} + \delta t\mathbf{J_3}),\ \mathbf{u^{n+1}} = \mathbf{u^n} + \frac{\delta t}{6}(\mathbf{J_1} + 2\mathbf{J_2} + 2\mathbf{J_3} + \mathbf{J_4}).$$

.

6. NUMERICAL RESULTS

The accuracy and efficiency of the proposed localized RBF-FD approach are tested using the following absolute error (AE), defined as

$$AE = \left| u^{\text{exact}} - u^{\text{approx}} \right|, \tag{6. 12}$$

where u^{approx} denotes the approximate solution and u^{exact} denotes the exact solution. Moreover, $\delta x = h = \frac{|b-a|}{N}$.

Now consider the following generalized Burgers-Fisher (gBF) equation:

$$u_t + \alpha u^\delta u_x - \nu u_{xx} = \beta u(1 - u^\delta), \text{ for } 0 < x < 1,\ t \geq 0, \tag{6. 13}$$

with the initial condition

$$u(x, 0) = \left[0.5 + 0.5 \tanh\left(\frac{-\alpha\delta}{2(1+\delta)}x\right)\right]^{\frac{1}{\delta}}. \tag{6. 14}$$

According to [24, 12, 26], the exact solution is given by

$$u^e(x,t) = \left[0.5 + 0.5\tanh\left(\frac{-\alpha\delta}{2(1+\delta)}\left(x - \left(\frac{\alpha}{1+\delta} + \frac{\beta(1+\delta)}{\alpha}\right)t\right)\right)\right]^{\frac{1}{\delta}}. \quad (6.\ 15)$$

On the domain $0 < x < 1$ and $0 < t < 1$, we analyze approximate solutions for $\beta = 0$, $\nu = 1$, $\alpha = 1$, and $\delta = 1, 2, 3$. Following [16], the gBF equation can be written as follows:

$$\frac{\partial u}{\partial t} - \nu\frac{\partial^2 u}{\partial x^2} + \beta u^{\delta}\frac{\partial u}{\partial x} - \gamma u(1-u^{\delta}) = 0, \text{ for } 0 \le x \le 1, \text{ and } t \ge 0, \quad (6.\ 16)$$

subject to the following initial condition:

$$u(x,0) = \left[0.5 + 0.5\tanh\{\frac{-\beta\delta x}{2(1+\delta)}\}\right]^{\frac{1}{\delta}} \quad (6.\ 17)$$

along with the boundary conditions:

$$u^e(0,t) = \left[0.5 + 0.5\tanh\{\frac{-\beta\delta}{2(1+\delta)}\{(\frac{\beta^2+\gamma(\delta+1)^2}{\beta(\delta+1)})t\}\}\right]^{\frac{1}{\delta}}, \quad (6.\ 18)$$

$$u^e(1,t) = \left[0.5 + 0.5\tanh\{\frac{-\beta\delta}{2(1+\delta)}, \{1 - (\frac{\beta^2+\gamma(\delta+1)^2}{\beta(\delta+1)})t\}\}\right]^{\frac{1}{\delta}}. \quad (6.\ 19)$$

The model equation (6. 16) gives rise to various forms of PDEs for different values of β, ν, γ, and δ. In particular, the generalized Burgers equation is obtained when $\gamma = 0$, and it reduces to the generalized Fisher equation when $\beta = 0$. The exact solution of equation (6. 16), derived by Chen and Zhang [4], is given as follows:

$$u^e(x,t) = \left[0.5 + 0.5\tanh\{\frac{-\delta\beta}{2(1+\delta)}\{x - (\frac{\beta^2+\gamma(\delta+1)^2}{(\delta+1)\beta})t\}\}\right]^{\frac{1}{\delta}}. \quad (6.\ 20)$$

We analyze approximate solutions for the parameter values $\beta = 0.0010, 0.10$, $\gamma = 0.0010$, $\nu = 1, 0.00250$, and $\delta = 1.0, 2.0, 4.0$.

6.1. **Example 1:** In this example, we consider the gBF equation (6. 13), where the parameters are $\alpha = 0.001$, $\beta = 0.001$ $\nu = 1$, equation (6. 14) represents the initial condition, while equation (6. 15) represents the boundary conditions and the analytical solution. For spatial step size $\Delta x = 0.10$ at time levels $t = 0.0010, 0.0050, 0.0100$ with temporal step size $\Delta t = 0.00010$ and $\delta = 1.0$, the absolute errors at nodes $x = 0.10, 0.50, 0.90$ are compared in Table 1. The existing numerical methods [21, 12, 24] are compared in Table 1 to provide a detailed comparison, which shows that the proposed method consistently outperforms existing techniques. Furthermore, a nearly perfect agreement between the numerical results and the analytical solution is a significant observation. The proposed method is also illustrated in Figure 1, where the corresponding surface plot further validates the approximate solution and the analytical and numerical profiles are in excellent agreement within graphical resolution.

TABLE 1. Comparison of the approximate solutions of gBF equation at time $t = 0.0010, 0.0050, 0.0100$, $x = 0.10, 0.50, 0.90$, $\beta = 0.0010$, $\alpha = 0.0010$, $\delta = 1.0$, $\nu = 1$, $\Delta t = 0.00010$ and $\Delta x = 0.10$ for Example 1.

x values	t values	Exact solution u^e	Approx. solution u	Approx. solution [21]	AE $\lvert u^e - u\rvert$	AE [21]	AE [12]	AE [24]
0.10	0.001	0.4999878	0.4999878	0.499988	9.8127×10^{-10}	1.97×10^{-8}	1.94×10^{-6}	2.25×10^{-8}
	0.005	0.4999888	0.4999888	0.499989	3.5107×10^{-9}	1.97×10^{-8}	9.69×10^{-6}	1.12×10^{-7}
	0.01	0.4999900	0.4999900	0.499990	5.4045×10^{-9}	1.97×10^{-8}	1.94×10^{-6}	2.25×10^{-7}
0.50	0.001	0.4999378	0.4999377	0.499938	1.0513×10^{-9}	3.58×10^{-9}	1.94×10^{-6}	4.58×10^{-8}
	0.005	0.4999388	0.4999387	0.499939	4.0146×10^{-9}	3.71×10^{-9}	9.69×10^{-6}	2.29×10^{-7}
	0.01	0.4999400	0.4999400	0.499940	6.5918×10^{-9}	3.88×10^{-9}	1.94×10^{-6}	4.58×10^{-7}
0.90	0.001	0.4999878	0.4999878	0.499988	9.8127×10^{-10}	1.97×10^{-8}	1.94×10^{-6}	2.25×10^{-8}
	0.005	0.4998888	0.4998888	0.499889	2.5164×10^{-9}	1.77×10^{-8}	9.69×10^{-6}	2.29×10^{-7}
	0.01	0.4998900	0.4998900	0.499890	3.0731×10^{-9}	1.74×10^{-8}	1.94×10^{-6}	4.58×10^{-7}

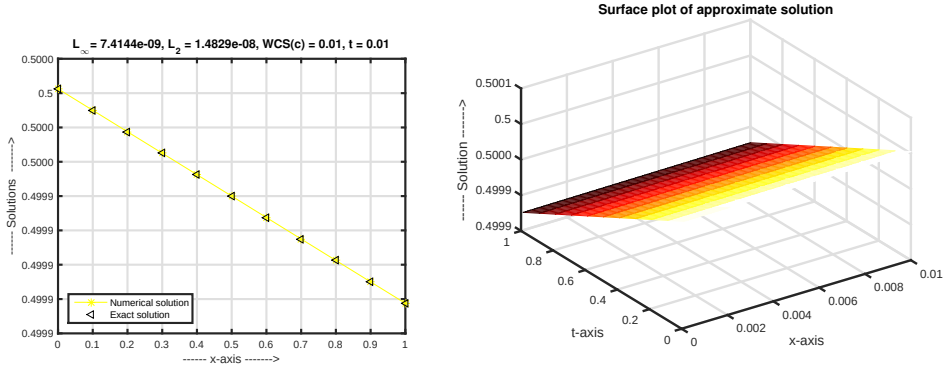

FIGURE 1. Example 1: Exact and approximate solutions (left) at time level $t = 0.010$, for $\beta = 0.0010$, $\alpha = 0.0010$, $\nu = 1$, and $\delta = 1.0$, with $\Delta t = 0.0001$ and $\Delta x = 0.10$, on the domain $[0, 1]$ using the proposed RBF-FD method. The right panel shows the surface plot of the approximate solution corresponding to equations (6. 13)-(6. 15).

6.2. **Example 2:** In this example, we consider the gBF equation (6. 13), where the parameters are $\beta = 1.0$, $\alpha = 1.0$, $\nu = 1$, the initial condition is represented by equation (6. 14), and the boundary conditions and analytical solution are represented by (6. 15). The absolute errors at the spatial coordinates $x = 0.10, 0.50, 0.90$, $\Delta t = 0.000010$, $\Delta x = h = 0.10$, $\delta = 2.0$ and $t = 0.00010, 0.00050, 0.0010$ are compared in Table 2. The proposed method consistently outperforms the existing methods, as demonstrated by the extensive comparison with some of the most sophisticated numerical techniques [21, 12, 24] in Table 2. The agreement between the analytical and numerical solutions is an important observation. In Figure 2, the proposed method is further illustrated. The surface plot verifies the accuracy of the approximate solution, indicating that the exact and numerical profiles are almost identical within the plotting resolution.

TABLE 2. Evaluating the approximate solutions of gBF equation at $x = 0.10, 0.50, 0.90$, $t = 0.00010, 0.00050, 0.0010$, $\alpha = 1.0$, $\nu = 1$, $\beta = 1.0$, $\delta = 2.0$, $\Delta x = 0.10$, and $\Delta t = 0.000010$ for Example 2.

x values	t values	Exact solution u^e	Approx. solution u	Approx. solution [21]	AE $\lvert u^e - u\rvert$	AE [21]	AE [12]	AE [24]
0.10	0.0001	0.6952661	0.6952661	0.695267	1.6934×10^{-8}	1.08×10^{-6}	2.80×10^{-4}	1.17×10^{-5}
	0.0005	0.6954258	0.6954257	0.695427	8.0027×10^{-8}	1.08×10^{-6}	1.40×10^{-3}	5.87×10^{-5}
	0.001	0.6956252	0.6956251	0.695626	1.4972×10^{-7}	1.08×10^{-6}	2.80×10^{-3}	1.17×10^{-4}
0.50	0.0001	0.6461299	0.6461299	0.646129	1.6855×10^{-10}	1.14×10^{-6}	2.69×10^{-4}	5.33×10^{-5}
	0.0005	0.6462972	0.6462972	0.646296	7.5973×10^{-10}	1.14×10^{-6}	1.34×10^{-3}	1.06×10^{-5}
	0.001	0.6465062	0.6465062	0.646505	1.3723×10^{-9}	1.14×10^{-6}	2.69×10^{-3}	1.06×10^{-5}
0.90	0.0001	0.5953105	0.5953105	0.595306	1.6309×10^{-8}	4.12×10^{-6}	2.55×10^{-4}	9.29×10^{-6}
	0.005	0.5954813	0.5954813	0.595477	7.6976×10^{-8}	4.12×10^{-6}	1.27×10^{-3}	4.64×10^{-5}
	0.001	0.5956948	0.5956949	0.595691	1.4383×10^{-7}	4.12×10^{-6}	2.55×10^{-3}	9.29×10^{-4}

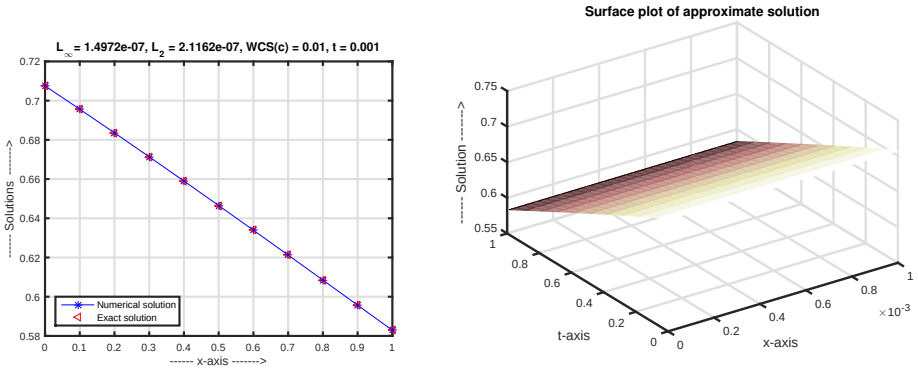

FIGURE 2. Exact and approximate solutions for Example 2 (left) at time $t = 0.010$, with parameters $\beta = 1.0$, $\nu = 1$, $\alpha = 1.0$, $\delta = 2.0$, $\Delta x = 0.10$, and $\Delta t = 0.00001$, using the proposed RBF-FD method on the domain $[0, 1]$. The right panel shows the corresponding surface plot of the approximate solution related to equations (6. 13)-(6. 15).

6.3. **Example 3:** For this case, we consider the gBF equation (6. 13), where the parameters are $\beta = 0.10$, $\alpha = 0.1$ $\nu = 1$, the initial condition is represented by equation (6. 14), and the boundary conditions and exact solution are represented by (6. 15). Table 3 presents the absolute errors for the temporal discretization using $\Delta t = 0.0010$, $\Delta x = 0.10$, $x = 0.20, 0.40, 0.60, 0.80$, $\delta = 1.0$ and $t = 0.10, 0.40, 0.80$. A thorough comparison with sophisticated numerical techniques [21, 26] in Table 3 demonstrates that the proposed method consistently performs better than current approaches. Furthermore, the excellent agreement between the approximate and exact solutions is an impressive and noteworthy result. The surface plot confirms the accuracy of the method, as shown in Figure 3, where the numerical and analytical profiles are nearly identical.

6.4. **Example 4:** In this example, the gBF equation (6. 13) is examined with equation (6. 14) representing the initial condition, (6. 15) representing the boundary conditions

TABLE 3. Absolute errors of the gBF equation at $x = 0.20, 0.40, 0.60, 0.80$, $t = 0.10, 0.40, 0.80$, with parameters $\beta = 0.10$, $\nu = 1$, $\alpha = 0.10$, $\Delta x = 0.10$, $\delta = 1.0$, and $\Delta t = 0.0010$ for Example 3.

t values	x values	Exact solution u^e	Approx. solution u	Approx. solution [21]	AE $\lvert u^e - u \rvert$	AE [21]	AE [26]
0.10	0.20	0.5000625	0.5000625	0.500062	5.2186×10^{-9}	5.98×10^{-8}	4.32×10^{-8}
	0.40	0.4975625	0.4975625	0.497562	1.0522×10^{-8}	3.95×10^{-8}	1.08×10^{-7}
	0.60	0.4950627	0.4950626	0.495063	2.8437×10^{-8}	1.97×10^{-8}	1.74×10^{-7}
	0.80	0.4925630	0.4925630	0.492563	1.8123×10^{-8}	9.80×10^{-10}	2.40×10^{-7}
0.40	0.20	0.5077494	0.5077494	0.507749	3.8040×10^{-10}	6.75×10^{-8}	3.85×10^{-7}
	0.40	0.5052498	0.5052498	0.505250	2.0129×10^{-8}	4.89×10^{-8}	6.65×10^{-7}
	0.60	0.5027500	0.5027499	0.502750	3.8674×10^{-8}	2.93×10^{-8}	1.71×10^{-6}
	0.80	0.5002500	0.5002500	0.500250	2.4650×10^{-8}	9.08×10^{-9}	2.76×10^{-6}
0.80	0.20	0.5179922	0.5179922	0.517992	7.7706×10^{-10}	5.09×10^{-8}	7.28×10^{-6}
	0.40	0.5154950	0.5154950	0.515495	2.1106×10^{-8}	4.27×10^{-8}	3.08×10^{-6}
	0.60	0.5129971	0.5129970	0.512997	4.0010×10^{-8}	3.09×10^{-8}	1.12×10^{-6}
	0.80	0.5104985	0.5104984	0.510498	2.5489×10^{-8}	1.63×10^{-8}	5.32×10^{-6}

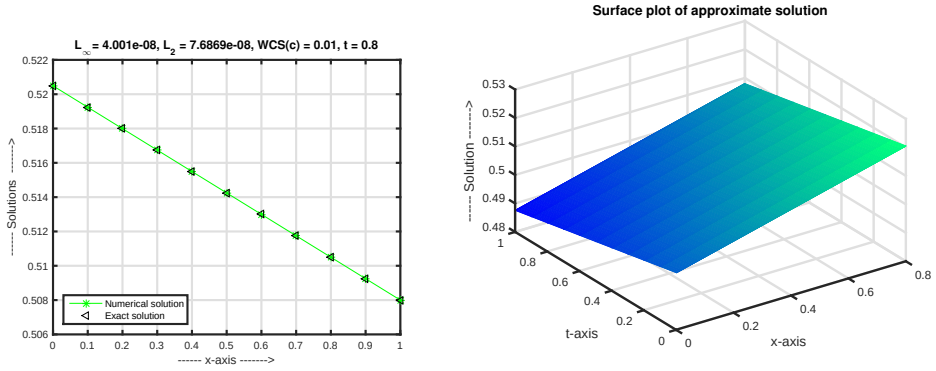

FIGURE 3. Example 3: the exact and approximate solutions (left) at time $t = 0.80$, $\beta = 0.10$, $\alpha = 0.10$, $\delta = 1.0$, $\nu = 1$, $\Delta x = 0.10$, and $\Delta t = 0.0010$ using the proposed RBF-FD method on the domain $[0, 1]$, as well as the surface plot of the approximate solution (right) corresponding to equations (6. 13)-(6. 15).

and exact solution, with parameters $\beta = 0.0$, $\nu = 1$, and $\alpha = 1.0$. Table 4 compares the absolute errors for temporal step size $\Delta t = 0.001$ and spatial step size $\Delta x = h = 0.10$ with $x = 0.10, 0.50, 0.90$, $t = 0.50, 1.0, 2.0$ and $\delta = 1.0$. As demonstrated in Table 4, the suggested approach produces better results than other numerical techniques [21, 12, 18], and the approximate and exact solutions show excellent agreement. The proposed method is further illustrated in Figure 4, where the surface plot confirms the great fidelity of the approximate solution due to the near-perfect overlap between the exact and numerical profiles within the plotting resolution.

TABLE 4. Evaluating the approximate solutions of the gBF equation at $x = 0.10, 0.50, 0.90$, $t = 0.50, 1.0, 2.0$ with parameters $\beta = 0.0$, $\nu = 1$, $\alpha = 1.0$, $\Delta x = 0.10$, $\delta = 1.0$ and $\Delta t = 0.0010$ for Example 4.

t values	x values	Exact solution	Approx. solution	Approx. solution	Approx. solution	Approx. solution	AE	AE	AE	AE
		u^e	u	[21]	[12]	[18]	$\lvert u^e - u \rvert$	[21]	[12]	[18]
0.50	0.10	0.5187412	0.5187408	0.518740	0.518741	0.518739	4.3615×10^{-7}	1.14×10^{-7}	6.34×10^{-8}	2.00×10^{-6}
	0.50	0.4687906	0.4687905	0.468791	0.468791	0.468790	8.9635×10^{-8}	1.13×10^{-7}	5.66×10^{-8}	1.00×10^{-6}
	0.90	0.4194577	0.4194581	0.419459	0.419458	0.419449	3.6375×10^{-7}	1.56×10^{-6}	4.12×10^{-8}	9.00×10^{-6}
1.0	0.10	0.5498340	0.5498336	0.549833	0.549832	0.549831	4.3362×10^{-7}	1.17×10^{-7}	2.02×10^{-6}	3.00×10^{-6}
	0.50	0.5000000	0.4999999	0.499999	0.499998	0.499998	8.7905×10^{-8}	3.79×10^{-8}	1.84×10^{-6}	2.00×10^{-6}
	0.90	0.4501660	0.4501664	0.450167	0.450165	0.450157	3.7845×10^{-7}	1.28×10^{-6}	1.37×10^{-6}	9.00×10^{-6}
2.0	0.10	0.6106392	0.6106388	0.610638	0.610575	0.610635	3.8879×10^{-7}	8.44×10^{-7}	6.42×10^{-5}	4.00×10^{-6}
	0.50	0.5621765	0.5621764	0.562176	0.562116	0.562175	7.7930×10^{-8}	1.16×10^{-7}	6.06×10^{-5}	2.00×10^{-6}
	0.90	0.5124974	0.5124978	0.512498	0.512450	0.512488	3.7161×10^{-7}	9.72×10^{-7}	4.75×10^{-5}	9.00×10^{-6}

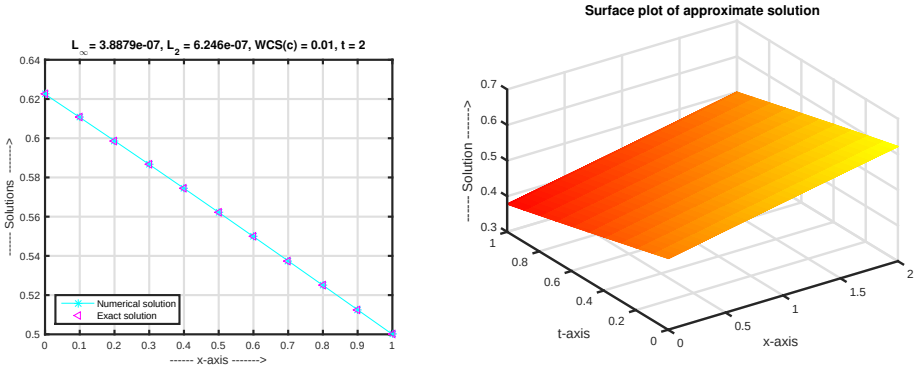

FIGURE 4. Example 4: Exact and approximate solutions (left) at time $t = 2.0$, $\beta = 0.0$, $\nu = 1$, $\alpha = 1.0$, $\delta = 1.0$, $\Delta x = 0.10$, and $\Delta t = 0.0010$ using the proposed RBF-FD method on the domain $[0, 1]$, along with the surface plot of the approximate solution (right) corresponding to equations (6. 13)-(6. 15).

6.5. **Example 5:** Here, we consider the gBF equation (6. 13), where $\beta = 0.0$, $\nu = 1$, $\alpha = 1.0$ are the parameters, equation (6. 14) represents the initial condition, and (6. 15) represents the boundary conditions and exact solution. Table 5 compares the absolute errors at time levels $t = 0.50, 1.0, 2.0$ for temporal step size $\Delta t = 0.0010$ and spatial step size $\Delta x = 0.10$, at $x = 0.10, 0.50, 0.90$ with $\delta = 2.0$. The proposed method is superior to existing numerical techniques [21, 12, 18], and the approximate solution shows excellent agreement with the exact solution. Figure 5 provides a clear illustration of the effectiveness of the proposed approach. The surface plot shows the high accuracy of the approximate solution due to the near-perfect overlap between the numerical and exact profiles within the plotting resolution.

6.6. **Example 6:** In this example, we consider the gBF equation (6. 16), with parameters $\beta = 0.0010$, $\nu = 1$, and $\gamma = 0.0010$. The boundary conditions and exact solution are represented by (6. 18)-(6. 19), while the initial condition is given in (6. 17). Table 6

TABLE 5. Approximate solutions of the gBF equation at $x = 0.10, 0.50, 0.90$ and $t = 0.50, 1.0, 2.0$ for Example 5 with parameters $\alpha = 1.0$, $\nu = 1$, $\beta = 0.0$, $\delta = 2.0$, $\Delta x = 0.10$, and $\Delta t = 0.0010$.

t values	x values	Exact solution	Approx. solution	Approx. solution	Approx. solution	Approx. solution	AE	AE	AE	AE
		u^e	u	[21]	[12]	[18]	$\|u^e - u\|$	[21]	[12]	[18]
0.50	0.10	0.5187412	0.5187408	0.518740	0.518741	0.518739	4.3615×10^{-7}	1.14×10^{-7}	6.34×10^{-8}	2.00×10^{-6}
	0.50	0.4687906	0.4687905	0.468791	0.468791	0.468790	8.9635×10^{-8}	1.13×10^{-7}	5.66×10^{-8}	1.00×10^{-6}
	0.90	0.4194577	0.4194581	0.419459	0.419458	0.419449	3.6375×10^{-7}	1.56×10^{-6}	4.12×10^{-8}	9.00×10^{-6}
1.0	0.10	0.5498340	0.5498336	0.549833	0.549832	0.549831	4.3362×10^{-7}	1.17×10^{-7}	2.02×10^{-6}	3.00×10^{-6}
	0.50	0.5000000	0.4999999	0.499999	0.499998	0.499998	8.7905×10^{-8}	3.79×10^{-8}	1.84×10^{-6}	2.00×10^{-6}
	0.90	0.4501660	0.4501664	0.450167	0.450165	0.450157	3.7845×10^{-7}	1.28×10^{-6}	1.37×10^{-6}	9.00×10^{-6}
2.0	0.10	0.7702837	0.7702834	0.770277	0.770272	0.770286	3.4446×10^{-7}	7.21×10^{-6}	1.18×10^{-5}	2.00×10^{-6}
	0.50	0.7264635	0.7264635	0.726456	0.726449	0.726469	5.3649×10^{-8}	7.35×10^{-6}	1.49×10^{-5}	5.00×10^{-6}
	0.90	0.6791092	0.6791096	0.679101	0.679095	0.679110	4.0713×10^{-7}	8.03×10^{-6}	1.43×10^{-5}	1.00×10^{-6}

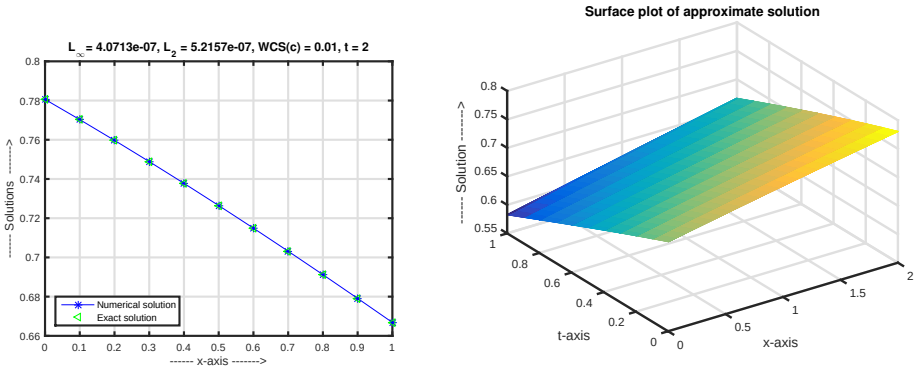

FIGURE 5. Example 5: Exact and approximate solutions (left) at time $t = 2.0$, $\beta = 0.0$, $\alpha = 1.0$, $\nu = 1$, $\delta = 2.0$, $\Delta x = 0.10$, and $\Delta t = 0.0010$ using the proposed RBF-FD method on the domain $[0, 1]$, along with the surface plot of the approximate solution (right) corresponding to equations (6. 13)-(6. 15).

compares the absolute errors at time levels $t = 0.50, 1.0, 2.0$ for temporal step size $\Delta t = 0.0010$ and spatial step size $\Delta x = 0.10$, at $x = 0.10, 0.50, 0.90$ with $\delta = 2.0$. The proposed method outperforms existing numerical methods [37, 3], as shown in Table 6, with the approximate results showing excellent agreement with the exact solution. The effectiveness of the proposed approach is demonstrated in Figure 6, where the exact and numerical solutions nearly coincide.

6.7. **Example 7:** Finally, we consider the gBF equation (2. 1), for which the exact solution is unknown. The initial and boundary conditions are defined as (see [11, 22]):

$$f(x) = \exp(-40x^2), \quad -1 \leq x \leq 1, \tag{6. 21}$$

with boundary conditions

$$U(\pm 1, t) = 0, \quad t > 0. \tag{6. 22}$$

TABLE 6. Approximate solutions of the gBF equation at $x = 0.10, 0.50, 0.90$ and $t = 0.50, 1.0, 2.0$ for Example 6 with parameters $\beta = 0.10$, $\nu = 1$, $\gamma = -0.0025$, $\delta = 2.0$, $\Delta x = 0.10$, and $\Delta t = 0.00010$.

t values	x values	Exact solution	Approx. solution	AE	AE	AE
		u^e	u	$\|u^e - u\|$	[37]	[3]
0.10	0.10	0.7058781	0.7058781	1.5265×10^{-8}	1.21×10^{-5}	9.47×10^{-6}
	0.50	0.7011405	0.7011405	3.1555×10^{-8}	2.90×10^{-5}	2.74×10^{-8}
	0.90	0.6963728	0.6963728	1.0324×10^{-8}	1.54×10^{-5}	9.57×10^{-6}
0.50	0.10	0.7056813	0.7056813	1.1563×10^{-8}	1.67×10^{-5}	9.58×10^{-6}
	0.50	0.7009424	0.7009424	4.4382×10^{-8}	4.69×10^{-5}	5.18×10^{-8}
	0.90	0.6961735	0.6961735	1.4597×10^{-8}	1.71×10^{-5}	9.66×10^{-6}
2.0	0.10	0.7049429	0.7049429	1.1488×10^{-8}	-	9.59×10^{-6}
	0.50	0.7001993	0.7001992	4.4584×10^{-8}	-	5.26×10^{-8}
	0.90	0.6954258	0.6954257	1.4662×10^{-8}	-	9.67×10^{-6}

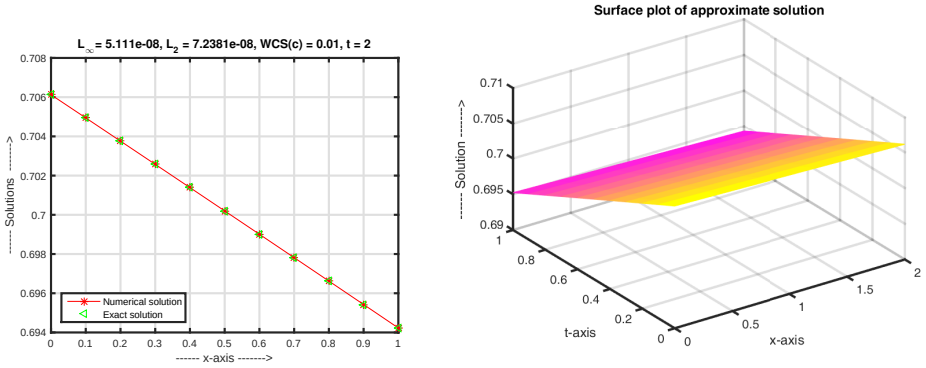

FIGURE 6. Evaluating the approximate solutions of the gBF equation at $x = 0.10, 0.50, 0.90$ and $t = 0.50, 1.0, 2.0$ with parameters $\gamma = -0.0025$, $\nu = 1$, $\beta = 0.10$, $\delta = 2.0$, $\Delta x = 0.10$, and $\Delta t = 0.00010$ for Example 6 corresponding to equations (6. 16)-(6. 19).

The computational parameters are selected as $N = 40$, $\Delta x = 0.05$, $\Delta t = 1.5/51$ for consistency with the results reported in [11, 22]. The parameter set used is $\alpha = 0$, $\nu = 0.1$, $\beta = 1$, $\delta = 1$. The proposed RBF-FD method successfully compute the approximate numerical solution for the considered parameter values as shown in Figure 7. The obtained results are found to be in good agreement with those reported in [11, 22], where the authors have presented similar graphical behaviors for the approximate solutions.

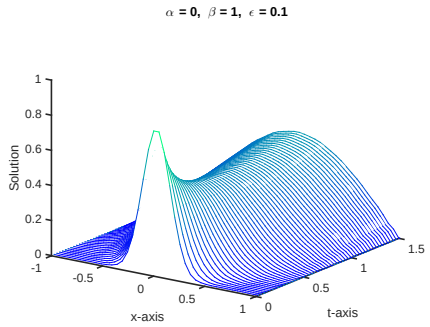

FIGURE 7. Approximate solution of the gBF equation at $N = 40$ and $t = 1.5$ with parameters values $\alpha = 0$, $\nu = 0.1$, $\beta = 1$, $\delta = 1$, $\Delta x = 0.05$ and $\Delta t = 1.5/51$ for Example 7 corresponding to equation (2. 1).

7. CONCLUSION

This work presents a numerical investigation of radial basis function (RBF) methods for the generalized Burgers-Fisher (gBF) equation. A hybrid meshless scheme based on the radial basis function-finite difference (RBF-FD) approach is developed for solving the model problem. Several nonlinear test cases of the gBF equation are successfully solved, demonstrating the capability of the method to handle nonlinear reaction-diffusion behavior. Time integration is performed using the fourth-order Runge-Kutta (RK-4) method. The accuracy of the proposed scheme is evaluated using the L_2 and L_∞ error norms, absolute errors, and graphical comparisons. Numerical results indicate improved accuracy compared with existing methods, along with a simple and efficient computational structure. The method also exhibits stability, good convergence behavior, and flexibility for a wide class of PDEs.

CREDIT AUTHORSHIP CONTRIBUTION'S STATEMENT

Hameed Ullah Jan : Conceptualization of the study, formulation of the mathematical model, development of the RBF–FD numerical scheme, supervision of the research work, manuscript writing, and final approval.

Hafeez Ullah: Implementation of the numerical algorithm, coding, computational experiments, data analysis, and preparation of numerical results.

Muhammad Rafiq: Literature review, validation of numerical results, comparison with existing methods, and proofreading of the manuscript.

Zakia Qureshi: Theoretical support, verification of mathematical derivations, graphical visualization, and formatting of the manuscript.

DECLARATIONS

Conflict of Interest: The authors declare that they have no conflicts of interest to report regarding the present study.
Funding: The authors received no financial support for this research, authorship, and publication of this article.
Acknowledgments: All the authors are thankful to the anonymous reviewers for their constructive comments, and also very thankful to the Chief editor, Punjab University Journal of Mathematics that she has given us a chance to improve our article up to the standard and able to publish.

REFERENCES

[1] V. Bayona, M. Moscoso, M. Carretero, and M. Kindelan. RBF-FD formulas and convergence properties. Journal of Computational Physics, **229**, No. 22 (2010): 8281–8295.
[2] A. G. Bratsos. An improved second-order numerical method for the generalized Burgers–Fisher equation. The ANZIAM Journal, **54**, No. 3 (2013): 181–199.
[3] A. G. Bratsos and A. Q. M. Khaliq. An exponential time differencing method of lines for Burgers-Fisher and coupled Burgers equations. Journal of Computational and Applied Mathematics, **356** (2019): 182–197.
[4] H. Chen and H. Zhang. New multiple soliton solutions to the general Burgers-Fisher equation and the Kuramoto-Sivashinsky equation. Chaos, Solitons & Fractals, **19**, No. 1 (2004): 71–76.
[5] Y. Chen, J. Lee, and A. Eskandarian. An overview on meshless methods and their applications. Meshless Methods in Solid Mechanics (2006): 55–67.
[6] E. W. Cheney and W. A. Light. A course in approximation theory. American Mathematical Society, Volume 101 (2009).
[7] M. E. Chenoweth. A local radial basis function method for the numerical solution of partial differential equations. (2012).
[8] G. Fasshauer and M. McCourt. Kernel-based Approximation Methods using Matlab. World Scientific Publishing Co Inc (2015).
[9] N. Flyer and G. B. Wright. A radial basis function method for the shallow water equations on a sphere. Proceedings of the Royal Society A, **465**, No. 2106 (2009): 1949–1976.
[10] C. Franke and R. Schaback. Convergence order estimates of meshless collocation methods using radial basis functions. Advances in Computational Mathematics, **8** (1998): 381–399.
[11] M. Hussain and S. Haq. Numerical solutions of strongly non-linear generalized Burgers–Fisher equation via meshfree spectral technique. International Journal of Computer Mathematics, **98**, No. 9 (2021): 1727–1748.
[12] H. N. A. Ismail, K. Raslan, and A. A. Abd Rabboh. Adomian decomposition method for Burgers-Huxley and Burgers-Fisher equations. Applied Mathematics and Computation, **159**, No. 1 (2004): 291–301.
[13] H. U. Jan and M. Uddin. Approximation and eventual periodicity of generalized Kawahara equation using RBF–FD method. Punjab Univ. J. Math., **53**, No. 9 (2021).
[14] H. U. Jan, M. Uddin, T. Abdeljawad, and M. Zamir. Numerical study of high order nonlinear dispersive PDEs using different RBF approaches. Applied Numerical Mathematics, **182** (2022): 356–369.
[15] H. U. Jan, I. A. Shah, N. U. Tamheeda, and A. Ullah. Approximation of nonlinear Sine–Gordon equation via RBF–FD meshless approach. Punjab Univ. J. Math, **55**, No. 9 (2023): 357–370.
[16] R. Kaur, Shallu, S. Kumar, and V. K. Kukreja. Numerical approximation of generalized Burgers-Fisher and generalized Burgers-Huxley equation by compact finite difference method. Advances in Mathematical Physics (2021).
[17] D. Kaya and S. M. El-Sayed. A numerical simulation and explicit solutions of the generalized Burgers–Fisher equation. Applied Mathematics and Computation, **152**, No. 2 (2004): 403–413.
[18] A. J. Khattak. A computational meshless method for the generalized Burgers-Huxley equation. Applied Mathematical Modelling, **33**, No. 9 (2009): 3718–3729.
[19] E. Larsson, B. Mavric, A. Michael, and F. Pooladi. A numerical investigation of some RBF-FD error estimates. Dolomites Research Notes on Approximation, **15**, No. 5 (2022): 78–95.

[20] F. Linares and G. Ponce. Introduction to nonlinear dispersive equations. SIAM (2014).
[21] S. A. Malik, I. M. Qureshi, M. Amir, A. N. Malik, and I. Haq. Numerical solution to generalized Burgers-Fisher equation using exp-function method hybridized with heuristic computation. PLoS One, **10**, No. 3 (2015): e0121728.
[22] R. C. Mittal and A. Tripathi. Numerical solutions of generalized Burgers–Fisher and generalized Burgers–Huxley equations using collocation of cubic B-splines. International Journal of Computer Mathematics, **92**, No. 5 (2015): 1053–1077.
[23] N. D. K. Mudiyanselage, J. Blazejewski, B. Ong, and C. Piret. A radial basis function-finite difference and parareal framework for solving time dependent partial differential equations. Dolomites Research Notes on Approximation, **15**, No. 5 (2022).
[24] R. Nawaz, H. Ullah, S. Islam, and M. Idrees. Application of optimal homotopy asymptotic method to Burger equations. Journal of Applied Mathematics (2013).
[25] R. B. Platte and T. A. Driscoll. Eigenvalue stability of radial basis function discretizations for time-dependent problems. Computers & Mathematics with Applications, **51**, No. 8 (2006): 1251–1268.
[26] M. M. Rashidi, D. D. Ganji, and S. Dinarvand. Explicit analytical solutions of the generalized Burger and Burger-Fisher equations by homotopy perturbation method. Numerical Methods for Partial Differential Equations, **25**, No. 2 (2009): 409–417.
[27] M. Z. Raza, M. Sadaf, G. Akram, and M. A. Iqbal. Nonlinear dynamical analysis of the neuron model with soliton structures and qualitative behavior. Nonlinear Dynamics, **114**, No. 4 (2026): 280.
[28] C. M. C. Roque, D. Cunha, C. Shu, and A. J. M. Ferreira. A local radial basis functions-finite differences technique for the analysis of composite plates. Engineering Analysis with Boundary Elements, **35**, No. 3 (2011): 363–374.
[29] U. Saeed and K. Gilani. CAS wavelet quasi-linearization technique for the generalized Burger-Fisher equation. Mathematical Sciences, **12**, No. 1 (2018): 61–69.
[30] Y. V. S. S. Sanyasiraju and G. Chandhini. Local radial basis function based gridfree scheme for unsteady incompressible viscous flows. Journal of Computational Physics, **227**, No. 20 (2008): 8922–8948.
[31] B. Sarler and R. Vertnik. Meshfree explicit local radial basis function collocation method for diffusion problems. Computers & Mathematics with Applications, **51**, No. 8 (2006): 1269–1282.
[32] S. A. Sarra. A numerical study of the accuracy and stability of symmetric and asymmetric RBF collocation methods for hyperbolic PDEs. Numerical Methods for Partial Differential Equations, **24**, No. 2 (2008): 670–686.
[33] S. A. Sarra and E. J. Kansa. Multiquadric radial basis function approximation methods for the numerical solution of partial differential equations. Advances in Computational Mechanics, **2**, No. 2 (2009): 220.
[34] R. Schaback. Error estimates and condition numbers for radial basis function interpolation. Advances in Computational Mathematics, **3**, No. 3 (1995): 251–264.
[35] Y. Y. Shan, C. Shu, and N. Qin. Multiquadric finite difference (MQ-FD) method and its application. Advances in Applied Mathematics and Mechanics, **1**, No. 5 (2009): 615–638.
[36] Y. Shang and Q. Chen. The generalized Cole-Hopf transformation for a generalized Burgers-Fisher equation with spatiotemporal variable coefficients. Applied Mathematics Letters, **117** (2021): 107074.
[37] M. Sari, G. Gurarslan, and I. Dag. A compact finite difference method for the solution of the generalized Burgers-Fisher equation. Numerical Methods for Partial Differential Equations, **26**, No. 1 (2010): 125–134.
[38] G. Stoyan and M. K. Jain. Numerical Solution of Differential Equations. Wiley Eastern Limited (1979).
[39] H. Tariq, M. Sadaf, G. Akram, and H. Ashraf. Construction of travelling wave solutions to new coupled Konno–Oono equation arising in magnetic field. International Journal of Modern Physics C (2025): 2750019.
[40] T. Tao. Nonlinear Dispersive Equations: Local and Global Analysis. AMS (2006).
[41] A. I. Tolstykh. On using RBF-based differencing formulas for unstructured and mixed structured-unstructured grid calculations. Proceedings of IMACS World Congress (2000): 4606–4624.
[42] L. N. Trefethen. Spectral Methods in MATLAB. SIAM (2000).
[43] M. Vivas-Cortez, G. Akram, M. Sadaf, S. Arshed, M. Abbas, and Y. S. Hamed. New applications of the fractional derivatives to extract abundant soliton solutions of the fractional Estevez–Mansfield equation in mathematical physics. Fractals, **34**, No. 2 (2026): 2540203–4.
[44] H. Wendland. Error estimates for interpolation by compactly supported radial basis functions of minimal degree. Journal of Approximation Theory, **93**, No. 2 (1998): 258–272.

[45] H. Wendland. Fast evaluation of radial basis functions: Methods based on partition of unity. Wavelets, Splines and Applications (2002).
[46] S. N. Chandler-Wilde and S. Langdon. A Galerkin boundary element method for high frequency scattering by convex polygon. SIAM Journal on Numerical Analysis, **45**, No. 2 (2007): 610–640.
[47] G. B. Wright. Radial basis function interpolation numerical and analytical developments. (2003).
[48] G. B. Wright and B. Fornberg. Scattered node compact finite difference-type formulas generated from radial basis functions. Journal of Computational Physics, **212**, No. 1 (2006): 99–123.